FEA- Aided Design, Optimization and Development of an Axial Flux Motor for Implantable Ventricular Assist Device

Neethu S., Shinoy K.S. and A.S. Shajilal

Abstract—This paper presents the optimal design and development of an axial flux motor for blood pump application. With the design objective of maximizing the motor efficiency and torque, different topologies of AFPM machine has been examined. Selection of optimal magnet fraction, Halbach arrangement of rotor magnets and the use of Soft Magnetic Composite (SMC) material for the stator core results in a novel motor with improved efficiency and torque profile. The results of the 3D Finite element analysis for the novel motor have been shown.

Keywords—Axial flux motor, Finite Element Methods, Halbach array, Left Ventricular Assist Device, Soft magnetic composite.

I. INTRODUCTION

ADVANCED cardiac or Heart failure may cause a drop in the output of heart from its normal resting output of about 5 liters a minute to an output around 2 liters of blood per minute. As the output reaches this low level, the kidneys, liver, and brain become irreversibly damaged. The mechanical cardiac assistance in the form of artificial hearts and Left Ventricular Assist Devices (LVADs) has become very popular in recent years and has been suggested as therapeutic solution to Congestive Heart failure (CHF)[1]-[3]. LVADs are mechanical circulatory devices placed between left ventricle and aorta that take over the function of a failing heart either partially or completely [3]. The main requirements for a blood pump are small size less than 30 mm in diameter and 60 mm in length, with a high rotational speed greater than 5000 rpm. Among the different LVADs available, unique advantages including compact size, low power consumption, high power density and larger diameter to length ratio made Axial Flux Permanent Magnet motors, the best choice for blood pump.

The blood pump discussed in this paper, unlike other pumps, is completely isolated from the biological organs inside human body. For long-term implantation and to reduce the risk of infection, a non- intrusive transcutaneous power transfer [4], in which power can be transferred through the skin between two electromagnetic coils, is preferred. Thus the very common problems faced by the implantable blood pumps including

Neethu S. is an M.Tech Student in the Electrical Engineering Department of College of Engineering, Thiruvananthapuram, Kerala, India. (e-mail: neethu.cep@gmail.com).

K. S. Shinoy is with Vikram Sarabhai Space Centre (VSSC, ISRO), Thiruvananthapuram, Kerala, India. (e-mail:ks_shinoy@vssc.gov.in).

A. S. Shajilal is a Professor in the Department of Electrical Engineering, College of Engineering, Thiruvananthapuram, University of Kerala, India. (email: shajilalpadmam@gmail.com).

blood clot formation and stress to blood cells have also been eliminated.

In this paper, the different design factors available for the improvement of the existing motor's efficiency and torque has been considered. For investigating the various design schemes of AFPM motor, 3D finite element analysis [5] of magnetic fields has been done with the aid of OPERA software [6].

II. NOVEL DESIGN AND OPTIMIZATION

A. Existing motor

The existing motor for LVADs has single- sided AFPM topology with slotted stator [7]. The motor details and dimensions are given in Table I and Table II respectively.

TABLE I
EXISTING MOTOR DETAILS

Item	Value	Units
Number of phases	3	-
Number of stator slots	6	-
Number of rotor poles	8	-
Torque constant	10	Nmm/A
Rated voltage	12	V
Rated current	1	A
Rated torque	10	Nmm
Rated speed At no load On load (at 12V)	11000 4200-4800	rpm rpm
Blood flow rate (at 110 mm of Hg)	5	l/min

TABLE II
EXISTING MOTOR DIMENSIONS

Part	Item	Value	Units
Air gap	Air gap length	1.5	mm
Rotor	Magnet thickness	2.25	mm
	Magnet- keeper thickness	1.5	mm
	Inner diameter	10	mm
	Outer diameter	24.5	mm
Stator	Length of stator teeth	13.5	mm
	Core thickness	4	mm
	Outer diameter	29	mm

Permendur is used for stator core and rotor magnets are made of Samarium cobalt (SmCo).The complete impeller system was tested in animals and the motor efficiency is calculated using (1).

$$\eta_{rated} = \frac{T_{rated} \times \omega_{rated}}{(T_{rated} \times \omega_{rated}) + P_{core} + P_{cu} + P_s} \times 100\% \quad (1)$$

Here the efficiency is calculated at the rated torque T_{rated} and the rated speed ω_{rated}. The core loss, copper loss is denoted by P_{core} and P_{cu} respectively and the stray loss composed of windage and friction loss is denoted by P_s . For a normal load current of 1A and the motor winding resistance of 1.75 Ω, copper loss or I^2R loss equals 1.75 W. The motor core loss composed of eddy current loss (P_e) and hysteresis loss (P_h) can be calculated using (2), (3).

$$P_e = \frac{K_e B_m^2 f^2}{\rho} \quad (2)$$

$$P_h = \frac{K_h B_m^n f}{\rho} \quad (3)$$

Here,ρ denotes the density of the core material, f is the motor frequency and B_m is the operating flux density.For the permendur core properties given in Table III ,P_e and P_h are 3.44 W (around 50% of the total loss)and 0.035 W respectively.

TABLE III
PROPERTIES OF PERMENDUR CORE

Property	Value	Units
Resistivity	420	$\mu\Omega$-mm
Operating magnetic flux density	0.45	T
Density	8200	Kg/m^3
Volume	2.64×10^{-6}	m^3
Hysteresis constant (K_h)	106.09	-
Eddy current constant(K_e)	53.2	-

The motor efficiency calculated from (1) is around 42% only. Thus the major concern in this high frequency motor is the eddy current loss which results in excessive heating. So the novel design will be concentrating on reducing the eddy current loss and thus to increase the motor efficiency and also to improve the torque profile. The existing motor was modeled in Opera 3D for comparison and is shown in Fig. 1.
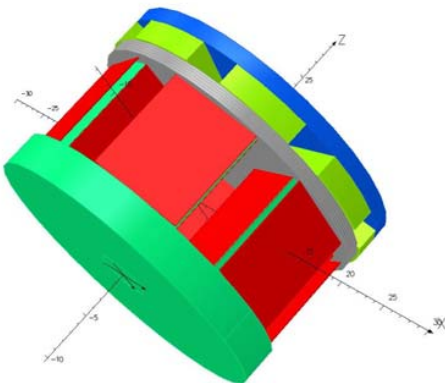

Fig. 1. Opera 3D model for the existing motor

B. Ideas of Novel Design and 3D Finite Element Analysis

With the design objective of maximizing motor efficiency and torque, keeping the motor dimensions and ratings same as in the existing motor, first attempt was to optimize the existing motor itself. The general design procedure for a typical BLDC motor was followed [8].Considering the application requirements (like peak torque, maximum speed, supply voltage, frequency, continuous power and torque requirement), novel design steps were done.

1) Single -sided AFPM motor with slotted stator: SmCo magnets are replaced by Neodymium Iron Boron (Nd-Fe-B) magnets owing to its high energy product (BHmax) and retentivity [9]. The number of stator slots and rotor poles are fixed as 6 and 8 respectively, considering the different factors including the speed of rotation, magnet material and grade, mechanical assembly of rotor and magnets, and the inertia requirements. The slot-pole combination affects cogging torque also [10]- [11]. The developed motor torque, T with N number of turns, current through each turn I , air gap flux density B, active length of the stator winding L and the average rotor radius r can be obtained from (4).

$$T = (NBIL) \times r \quad (4)$$

From (4), the torque developed by the motor increases as the air gap flux density is increased. Thus we need to increase the air gap flux density for maximizing the motor efficiency and torque.

In the novel motor, rotor magnets are arranged in Halbach array[7],[12].The halbach array has many advantages compared to conventional PM array[7].The possible halbach angles considered in this paper are 90°, 60° and 45°. Fig. 2 shows the magnetic potential vectors in the Opera 3D model for rotor magnets arranged in halbach 90°.
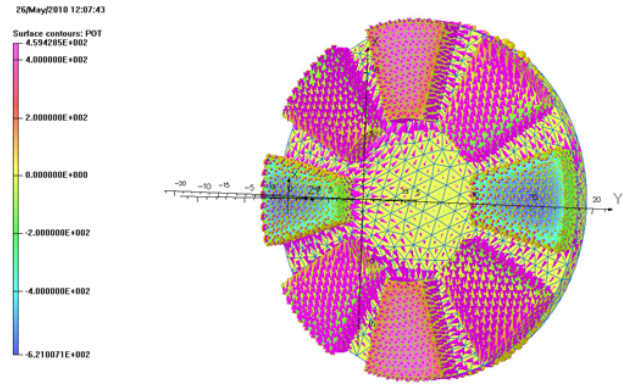

Fig. 2. Magnetic potential vectors in Opera 3D for halbach 90°

From the FE analysis, it is seen that as the angle between magnetic flux density vectors of the neighboring magnets decreases, peak value of normal component of $B(B_z)$ increases slightly as in Table IV. Thus halbach angle 45°, with maximum B_z is the optimal choice.

The self-shielding property (unique property of producing a strong periodic magnetic field on one side of array with a minimal field on opposite side of the array) of halbach

TABLE IV
PEAK B_z VALUES FOR HALBACH AND NON-HALBACH MODELS

Model	Peak B_z (T)
Non- halbach	0.5
Halbach 90°	0.51
Halbach 60°	0.49
Halbach 45°	0.61

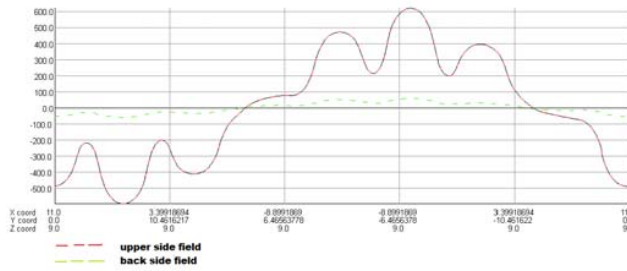arrangement is shown in Fig. 3. Thus the rotor back iron is not essential which improves the dynamic performance of the motor.

Fig. 3. Plot of magnetic potential in the upper side and back side of Halbach array

Actual torque and cogging torque of the motor was calculated using Opera for non- halbach and halbach models. Fig. 4. shows the actual torque and cogging torque waveforms plotted against the rotation angle of rotor for non-halbach model.

Table V gives the average values of torque for different models. For the sinusoidal torque waveform, the average torque (T_{avg}) is calculated from the peak torque (T_P) by (5).
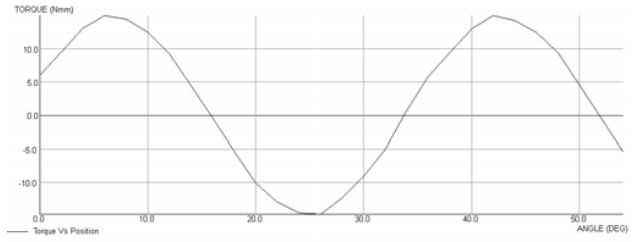
TABLE V
ACTUAL TORQUE AND COGGING TORQUE AVERAGE VALUES
FOR HALBACH MODELS

| Model	Actual Torque (Nmm)	Cogging Torque (Nmm)	Number of cycles (in 360° rotation)
Non -halbach	9.54	0.286	24
Halbach 90°	7.95	3.18	12
Halbach 60°	3.18	2.55	6
Halbach 45°	7	4.13	6

$$T_{avg} = T_p \times \frac{2}{\Pi} \qquad (5)$$

The cogging frequency (number of cycles in 360° rotation of rotor) has been reduced significantly in halbach 45° which reduces the core loss, but the magnitude of cogging torque is not easily acceptable.

2) Slotless Torus AFPM motor: The issues of cogging torque in the slotted stator can be solved by using the slotless topology and the motor torque can be improved by using double-sided AFPM topology. The slotless torus AFPM topology has been considered the superior one among the different double-sided AFPM topologies [13]. The torus topology has the stator disc with windings, placed in between two rotor discs on either side. The Opera 3D model for slotless torus

(a)
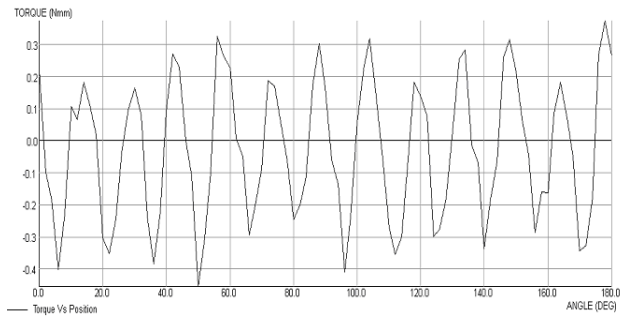
(b)

Fig. 4. Actual torque and cogging torque Vs. rotation angle of rotor disc in non-halbach model. (a) Actual torque Vs. rotation angle (b) Cogging torque Vs. rotation angle

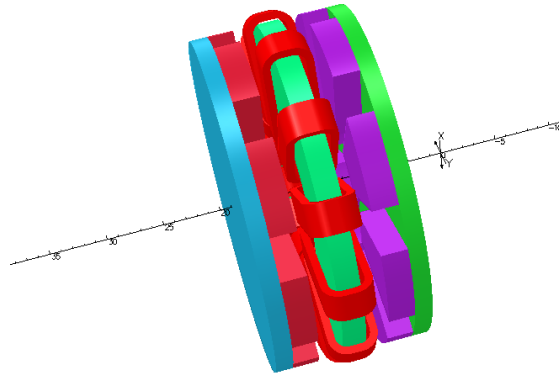is shown in Fig. 5. The slotless torus motor dimensions are given in Table VI.

Fig. 5. Opera 3D model for slotless torus AFPM motor

The total motor length is reduced to around 13mm, which is more compact. Currents in stator windings are shown in Fig. 6. The stator windings are energized in a fashion similar to BLDC motor, i.e., two phases energized at a time and the third phase not energized. Flux path in a slotless torus is shown in Fig. 7. As expected slotless torus motor torque is doubled [7], compared to the single- sided topology, which is seen in Fig. 8.

Magnet fraction or pole- pitch is an important design factor to be considered. For maximum utilization of the rotor magnets and to avoid the saturation effects in stator core, magnet

TABLE VI
SLOTLESS TORUS MOTOR DIMENSIONS

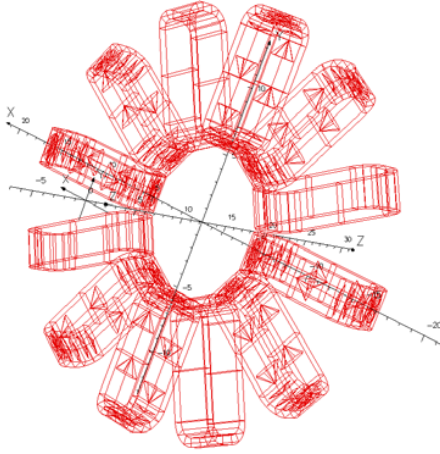| Part	Item	Value	Units
Air gap	Air gap length	1.5	mm
Rotor	Magnet thickness	2.25	mm
	Magnet- keeper thickness	1.5	mm
	Inner diameter	13.5	mm
	Outer diameter	29.5	mm
Stator	Core thickness	2	mm
	Outer diameter	29.5	mm

Fig. 6.   Currents in stator windings

fraction should be decided carefully [14].Different magnet fractions are considered for fixed stator core thickness and the results are given in Table VII. For e.g., if pole pitch = 75 %, then the magnet dimensions (outer magnet arc length, O_m and inner magnet arc length, I_m) are estimated using (6) and (7) respectively.

TABLE VII
ACTUAL TORQUE AVERAGE VALUES FOR DIFFERENT
MAGNET FRACTIONS

Pole-pitch (%)	Actual torque - average (Nmm)
65	10.9
70	11.5
74	12.8
75	13.71
76	13.4
77	13.45
79	13.5
80	13.6
85	13.6

$$O_m = \frac{2\Pi r_o}{8} \times (0.75) \qquad (6)$$

$$I_m = \frac{2\Pi r_i}{8} \times (0.75) \qquad (7)$$

Here r_o ,r_i is the outer and inner radius respectively of the rotor disc. The magnet dimensions for pole-pitch selection are shown in Fig. 9. From Table VII, pole-pitch of 75% is taken as the optimal value considering saturation effects also.
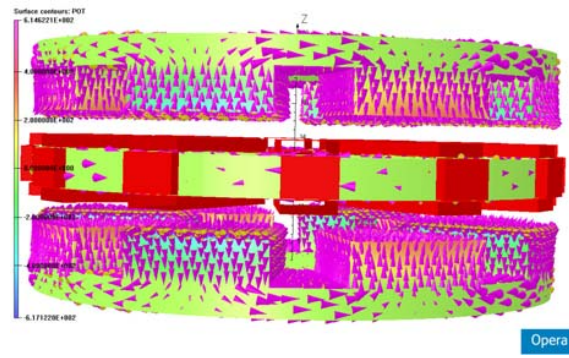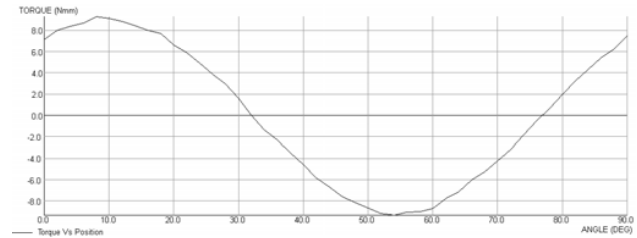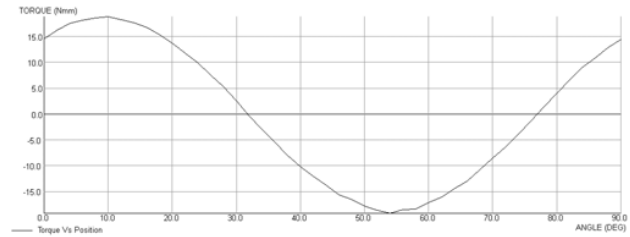

Fig. 7.   Flux path in Slotless torus

(a)

(b)

Fig. 8.   Actual torque comparison in single- sided AFPM and Slotless Torus a) Single -sided AFPM b) Slotless Torus

As discussed earlier, the major problem faced by this motor is the heating due to high frequency eddy currents. Soft magnetic composite (SMC) material in the novel motor will be replacing the permendur core in the existing motor. The unique properties of SMC core [7],[15]-[17] will definitely improve the efficiency of motor. The leading properties of the selected SMC material (Somaloy 700 HR 3P) are given in Table VIII. From Table VIII, it is clear that SMC is having very high resistivity, which in turn will improve the eddy current loss, which is the most dominant one at higher frequencies.

III. CONCLUSION

This paper discussed the different design issues of an AFPM motor for LVAD application. The design and optimization of the novel motor was done with the aid of a FE software, Opera and the 3D FEA results are shown. The novel motor torque is increased and the air gap flux density is also improved. The eddy current loss is reduced considerably (around 20%
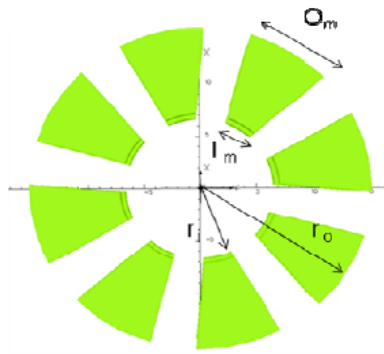
Fig. 9.   Pole- pitch selection- magnet dimensions

TABLE VIII
PROPERTIES OF SMC MATERIAL

Property	Value	Units
Resistivity	600	$\mu\Omega$-m
Coercivity	237	A/m
Magnetic flux density (at 10000 A/m)	1.57	T
Density	7.52	gm/cm^3
Core loss	301	W/Kg

of the total loss) by using SMC core. Thus the novel motor efficiency is expected to be around 78 %. For the experimental verification of these results, the novel motor will be fabricated and the in-vitro tests will be conducted in the due course of time.

ACKNOWLEDGMENT

REFERENCES

[1] L. Lockyer and M. Bury,"The construction of a modern epidemic: the implications for women of the gendering of coronary heart disease." *Journal of Advanced Nursing*, vol. 39, no. 5, 2002.

[2] Po-Lin Hsu and Richard McMahon."Design Method of an Innovative Motor for an Intra-Aortic Ventricular Assist Device," *IEEE Transactions*, 2010, pp. 1023-1028.

[3] M. Horz, H.-G. Herzog, and N. Mendler."System design and comparison of calculated and measured performance of a bearing less BLDC-drive with axial flux path for an implantable blood pump",*SPEEDAM* ,2006,pp.6-9.

[4] L. Zhao, C. F. Foo, and K. J. Tseng,"A new structure transcutaneous transformer for artificial heart," *IEEE Trans. Magn.*, vol. 35, pp.3350-3352, Sept. 1999.

[5] Joao Pedro A. Bastos and Nelson Sadowski. *Electromagnetic Modeling by Finite Element Methods*. Eastern Hemisphere Distribution, Marcel Dekker,Inc., 2003.

[6] Opera -2D and 3D User Guide, Cobham Technical Services, Vector Fields Software, Version 13.0, July 2009.

[7] Jacek F. Gieras, Rong- Jie Wang and Maarten J. Kamper. *Axial Flux Permanent Magnet Brushless Machines*. Springer Science + Business Media, Inc. Kluwer Academic Publishers, 2005.

[8] J. R. Hendershot Jr., T.J.E. Miller. *Design of Brushless Permanent magnet motors*. Magna Physics publishing and Clarendon press- Oxford 1994.

[9] Rahman, M.A.; Slemon, G.R. "Promising Application of Neodymium Boro Iron Magnets in Electrical Machines,". *IEEE Trans. on Magnetics*, vol. 21, No 5, September 1985. pp. 1712-1716

[10] Yon-Do Chun, Dae-Hyun Koo, Yun-Hyun Cho and Won-Young Cho. "Cogging Torque Reduction in a Novel Axial Flux PM Motor", *International Symposium on Power Electronics, Electrical Drives, Automation and Motion (SPEEDAM)*, 2006,pp. 16-19.

[11] Federico Caricchi, Fabio Giulii Capponi, Fabio Crescimbini and Luca Solero. "Experimental Study on Reducing Cogging Torque and No-Load Power Loss in Axial-Flux Permanent-Magnet Machines With Slotted Winding,". *IEEE Transactions on Industry Applications*, Vol. 40, No. 4, July/August 2004.pp. 1066-1075.

[12] Jacek F. Gieras, Mitchell Wing. *Permanent Magnet Motor Technology*. Eastern Hemisphere Distribution, Marcel Dekker,Inc., 2002.

[13] Metin Aydin, Surong Huang, and Thomas A. Lipo. "Torque Quality and Comparison of Internal and External Rotor Axial Flux Surface-Magnet Disc Machines", *IEEE Transactions on Industrial Electronics*, Vol. 53, No. 3, June 2006, pp. 822-829.

[14] P. Karutz, T. Nussbaumer, W. Gruber and J.W. Kolar. "Saturation Effects in High Acceleration Bearingless Motors". *IEEE Transactions*, 2008, pp. 472-477.

[15] P. Jansson, "SMC Materials - Including Present and Future Applications", PM2TEC Conference 2000, pp87-97

[16] A.G. Jack, B.C. Mecrow, G. Nord, P.G. Dickinson. "Axial Flux Motors Using Compacted Insulated Iron Powder and Laminations -Design and Test Results", *IEEE Transactions*, 2005, pp.378-385.

[17] Goga Cvetkovski, Lidija Petkovska, Milan Cundev, and Sinclair Gair. "Improved Design of a Novel PM Disk Motor by Using Soft Magnetic Composite Material,". *IEEE Transactions on Magnetics*, Vol. 38, No. 5, September, 2002, pp.3165-3167.